Developing an antisense oligonucleotide treatment for Spinocerebellar Ataxia Type 3

Toonen, L.J.A.

6

Intracerebroventricular administration of a 2-'O-methyl phosphorothioate antisense oligonucleotide results in activation of the innate immune system in mouse brain

Lodewijk J.A. Toonen*, João Casaca-Carreira*, Maria Pellisé-Tintoré, Hailiang Mei, Yasin Temel, Ali Jahanshahi#, Willeke M.C. van Roon-Mom# (2018).
***,# authors contributed equally**
Nucleic Acid Ther. doi:10.1089/nat.2017.0705

ABSTRACT

Antisense oligonucleotides (AONs) are versatile molecules that can be used to modulate gene expression by binding to RNA. The therapeutic potential of AONs appears particularly high in the central nervous system, due to excellent distribution and uptake in brain cells, as well as good tolerability in clinical trials thus far. Nonetheless, immune stimulation in response to AON treatment in the brain remains a concern. For this reason we performed RNA sequencing analysis of brain tissue from mice treated intracerebroventricularly with phosphorothioate, 2'O-methyl modified antisense oligonucleotides. A significant upregulation of immune system associated genes was observed in brains of AON treated mice, with the striatum showing largest transcriptional changes. Strongest upregulation was seen for the anti-viral enzyme 2'-5'-oligoadenylate synthase-like protein 2 (Oasl2) and Bone marrow stromal antigen 2 (Bst2). Histological analysis confirmed activation of microglia and astrocytes in striatum. The upregulation of immune system associated genes was detectable for at least two months after the last AON administration, consistent with a continuous immune response to the AON.

INTRODUCTION

Antisense oligonucleotides (AONs) are versatile molecules consisting of single strands of nucleic acids capable of binding to RNA through standard Watson-Crick interactions. AONs have been used since the 1960s [1], and a wide range of chemical modifications have been developed to tailor AONs to specific functions as well as improve their drug-like properties such as: binding energy, stability and tolerability [2]. Single-stranded AONs are mainly used for the down-regulation of target transcripts through an RNAse-H dependent mechanism, or to induce steric blocking for modulation of transcript splicing or translational inhibition [3]. Making use of these mechanisms, AONs are investigated as therapeutic agents for a wide range of diseases, and show particular promise for neurodegenerative disorders [3]. This is mainly due to the favourable distribution and excellent cellular uptake of AONs following administration in the cerebrospinal fluid (CSF) [4-6]. An AON approach based on redirecting splicing of SMN2 to induce protein expression as a treatment strategy for spinal muscular atrophy (SMA) [7, 8] has arguably been most successful thus far, with recent approval from the Food and Drug Administration (FDA) and European Medicines Agency (EMA) being achieved for the drug Spinraza [7]. AON-based therapies for other central nervous system (CNS) disorders have also shown very promising preclinical results in animal models, where for instance target downregulation for huntingtin [9] and SOD1 [10] protein was achieved very efficiently in mice. SOD1 downregulation was the first AON based therapy for the CNS to be successfully tested in phase 1 trial [11], and AON based downregulation of huntingtin as well as SOD1 are both in phase 2 clinical trial at the moment.

Most AONs currently in clinical development for CNS disorders contain a phosphorothioate (PS) backbone modification to provide protection from nuclease degradation, improve cellular uptake and to enhance AON stability [12]. Despite its many advantages, the main drawback of the PS backbone is its increased cellular toxicity compared to standard phosphodiester linkage [13]. These side effects may arise due to non-specific binding to proteins [14, 15] or complement activation [16]. Indeed, PS-AON are known to induce production of IL-6, TNF-α, IL-12 and CCL5 when added to splenocyte cultures [17]. At least some of these side effects also appear to occur in the CNS, where AON administration has been shown to induce an immune response in the rat brain [18]. This immune stimulation has a clear AON sequence dependent effect, which can be separate from RNA target engagement, as in particular the CpG motifs are known stimulants of the Toll-like receptor 9 (TLR) [19]. These immunostimulatory effects can fortunately be diminished by 2'-sugar and 5-methyl cytosine modifications [20-22], which also was shown to improve AON tolerability in the CNS [23].

Given the clinical advancement of AONs for disorders of the CNS, a comprehensive assessment of potential side effects is required. For this reason, we assessed the effect of a PS 2′-O-methyl modified AON when administered intracerebroventricularly (ICV) in the mouse brain. To assess changes induced at the transcript level, RNA sequencing analysis was performed for striatum, cortex and cerebellum. Furthermore, immunohistological examination was performed on striatal tissue to determine microglia and astrocyte activation after AON administration.

Table 1. overview of RNA sequencing samples from FVB test cohort

	PBS treated		AON treated	
cerebellum	n = 7	week 2: n = 4	n = 8	week 2: n = 6
		week 8: n = 3		week 8: n = 2
cortex	n = 8	week 2: n = 5	n = 7	week 2: n = 5
		week 8: n = 3		week 8: n = 2
striatum	n = 6	week 2: n = 2	n = 8	week 2: n = 5
		week 8: n = 4		week 8: n = 3

MATERIALS AND METHODS

Animals

Wild-type FVB mice and C57BL/6 mice were obtained from Jackson Laboratories (Bar Harbor, ME, USA). The test cohort of FVB mice used for RNA sequencing consisted of a total of 18 mice from 3 to 4 months of age, 3 of which received a total of 215 µg AON, 6 received 665 µg AON and 9 received PBS. The independent validation cohort consisted of 12 C57BL/6 mice, 8 of which received a total dose of 500 µg of the AON and 4 animals received PBS. Animal experiments were carried out in accordance with European Communities Council Directive 2010/63/EU and were approved by the Leiden University and Maastricht University animal ethical committees. Mice were housed individually during experimental procedures, with food and drinking water available *ad libitum* and with a reverse light/dark cycle of 12 h. Only male mice were used for experiments.

AON administration

The AON consisted of a 19-mer (5′- CUGAACUGGUCUACAGCUC –3′) [24, 25] and followed a steric blocking design with a full PS backbone and uniform 2'-O-methyl ribose modifications. Nucleotides were not 5-methyl modified. The AON was designed to be non-complementary to the mouse genome, with a maximum of 17/19 nucleotide complementarity. AONs were dissolved in sterile PBS without calcium or magnesium and diluted to a maximum concentration of 40 µg/µl for injection. Injections of AONs was performed ICV, following previously described procedures [24, 26]. In brief, mice were fixed in a stereotactic frame under isoflurane anaesthesia, and a burr hole was drilled in the skull. A 26 gauge cannula (Plastics1, Anaheim, CA, USA) was implanted at coordinates (relative to bregma) AP: –0.4, ML: 1.0, DV: –1.7 mm, and fixed with dental composite (OptiBond® All-In-One, Kerr Dental, Bioggio, Switzerland). AONs or PBS were administered under general anaesthesia at an infusion rate of ~ 1 µl/min for a total dose of 215 µg or 665 µg. The simplified administration scheme is depicted in (Fig. 1A). The 215 µg dose was achieved through a total of 6 injections (15 µg to 50 µg per injection) during a 2 month period. Animals dosed to 665 µg received 2 extra injection of 250 and 200 µg during a 1.5 month period. Animals from the C57Bl/6 validation cohort received repeated injections

of 5 µl of the same non-targeting AON at 20 µg/µl. Five injections for a total dose of 500 µg was performed in these mice during a 10 week period.

Tissue collection

Mice were sacrificed either 2 weeks (n = 11) or 8 weeks (n = 7) post injection (Fig. 1A). Mice from the C57Bl/6 validation cohort were sacrificed 4 months after the last AON injection (n = 12). Brains were removed, and striatum, cortex and cerebellum of the left hemisphere were snap frozen in liquid nitrogen and stored at -80 ˚C until RNA isolation. The entire right hemisphere was fixed in 4% paraformaldehyde overnight at 4 ˚C. Tissue was then placed in 30% sucrose for 1 or 2 days and stored in PBS containing 0.02% sodium azide at 4˚C until sectioning.

Immunofluorescent stainings and assessment of GFAP and Aif1 levels

Fixed mouse brain tissue was sectioned on a vibratome at 25 µm thickness, and coronal sections were collected in PBS containing 0.02% sodium azide. Sections were then washed with PBS containing 0.2% triton-X100 for 10 min and incubated overnight with one of the following primary antibodies diluted in 1% normal donkey serum: rabbit anti-PS-backbone (kind gift of Ionis Pharmaceuticals, Carlsbad, CA, USA; 1:1000), rabbit anti-glial fibrillary acidic protein (GFAP) (Dako; 1:1000), or rabbit anti-aif1 (Wako Chemicals USA, Inc ; 1:500). Sections were washed with PBS and incubated with secondary antibodies, donkey anti-rabbit-alexa Fluor 488 1:500 (Life technologies, Paisley, UK) for fluorescent optical density determination. After washing, sections were mounted on superfrost plus coated microscope slides (Fisher Emergo, Landsmeer, Netherlands). The slides were then immediately coverslipped using EverBrite hardset mounting medium with DAPI (Biotium, Hayward, USA). For cell morphology assessment, the sections were incubated overnight with the primary antibody with the same dilution, followed by a secondary antibody 1:800 biotinylated donkey anti-rabbit (Jackson Immunoresearch Laboratories, West Grove, USA), and ABC-step (avidin–biotin-peroxidase complex, diluted 1:800, Elite ABC-kit, (Vestastain, Burlingame, CA, USA). To visualize the horseradish peroxide reaction product, the sections were incubated with DAB (3,30-diaminobenzidine tetrahydrochloride) with nickel chloride intensification. Slides were washed, dehydrated and coverslipped using Pertex (Histolab Products ab, Goteborg, Sweden). Optical density determination through fluorescence was performed on three coronal sections per mouse (5 AON treated vs 5 PVS treated) at 10x magnification using Image J software. Coronal sections of the striatum at 60x magnification were scored for Aif1 levels to assess microglia activation and for GFAP levels to assess astrocytes number and state of activation. Morphology of cells was assessed for cells in 5 images from three different sections per mouse. The scoring of microglia activation state was done based on morphology assessment from previous studies [27, 28]. Aif1 positive cells (microglia) were categorized as resting or active state. Resting state microglia were characterized by small and smooth-surfaced cell bodies with thin, ramified processes. Active microglia had an irregularly shaped cell body with thicker, ramified processes. Activation of astrocytes was assessed similar to previously described [29]. Resting state astrocytes had low levels of GFAP expression, with

stellate morphology and numerous spatially distinct, thin branched processes. Active astrocytes had increased GFAP expression, with a hypertrophic appearance and thicker, highly branched, overlapping processes. Images of AON distribution were obtained as described previously [26].

RNA isolation and sequencing

RNA was isolated from mouse striatum, cortex and cerebellum using the Trizol method and PureLink RNA mini kit (Ambion, Thermo Fisher scientific, Waltham, MA, USA). Genomic DNA was degraded using a DNAse incubation according to manufacturer's protocol, and concentration and purity of RNA was determined by Nanodrop spectrophotometry. Library preparation and RNA sequencing was done at deCode Genetics (Reykjavik, Iceland). Starting material was approximately 1 μg of total RNA, with an average RIN value of 7.6 (SD ± 0.3). Quality of RNA was determined using the LabChip GX (Perkin Elmer, Waltham, USA). Sample preparation was performed non-strand specifically, using the TruSeq Poly-A v2 kit (Illumina, San Diego, USA). Capture of mRNA was performed with magnetic poly-T beads, followed by fragmentation. Synthesis of cDNA was then performed with random hexamer primers using the SuperScript II kit (Invitrogen, Carlsbad CA, USA). Subsequently, 2nd strand cDNA synthesis was performed in conjunction with RNAse-H treatment. Indexing adapters were ligated to the ds-cDNA and amplification was performed using PCR. Insert size and sample diversity was assessed through pool sequencing on a MiSeq instrument (Illumina). Sequencing (read length 2x125 cycles) was then performed using the HiSeq 2500 with v4 SBS sequencing kits. Illumina scripts (bcl2fastq v1.8) were used for demultiplexing and FASTQ file generation. Counts were aligned to genes of the mouse reference genome build 10 (GRCm38/mm10).

Analysis of differential gene expression

Analysis of gene expression was performed only on genes exceeding an average of >4 counts per million (CPM). Gene counts were normalized using the trimmed mean of M-values (TMM) normalization method [30]. Differential gene expression was performed using the R package edgeR, version 3.14.0 [31]. A principal component analysis was performed to assess clustering of samples per brain region, and 6 out of 53 samples were excluded based on abnormal clustering (Fig. S2A). One additional sample was excluded based on the fact that there was a large percentage of reads originating from a single gene (Fig. S2B). The design model matrix for edgeR was described as model.matrix(~ treatment_group * brainregion) to allow for detection of AON treatment effects at the transcript level accounting for the different brain regions. Dispersion was estimated using the design matrix, after which a generalized linear model (GLM) was fitted using the glmFit function. Likelihood ratio test was performed using the glmLRT function on the coefficients of AON treatment and the interaction term treatment*brainregion. To assess the effect of the AON treatment within each brain region, a coefficient was assigned for each brain region and treatment group. The glmLRT function was then performed with contrast argument to allow pairwise treatment effect comparison for each brain region. Genes were considered significantly differentially expressed when the false discovery rate (FDR, Benjamini-Hochberg) was below 0.05. Data was plotted using ggplot 2 or graphpad Prism version 7.0.

Pathway analysis

Genes found to be significantly differentially expressed between PBS and AON treated mice at FDR < 0.01 were included for pathway analysis using Ingenuity (Ingenuity Systems Inc., Redwood City, CA; www.ingenuity.com). Functional annotation of genes was performed using DAVID bioinformatics resources 6.8 (https://david.ncifcrf.gov). Pathways and biological processes with corrected p-value < 0.05 (Benjamini–Hochberg) were considered significantly enriched in the dataset.

Validation with ddPCR

To validate the RNA sequencing results, droplet digital PCR (ddPCR) was performed on striatum RNA from the same samples as used for RNA sequencing for the FVB test cohort, and using RNA from a separate C57Bl/6 validation cohort. cDNA was generated as previously described [32] using Transcriptor First Strand cDNA Synthesis Kit (Roche, Mannheim, Germany) with random hexamer primers. The amount of cDNA that was used per reaction was the equivalent of 30 ng of RNA for ddPCR for genes of interest. Due to high expression, 5 ng of input was used for reference genes. PCR product sizes ranged between approximately 100 and 200 bp (primer sequences are listed in Table S1). PCR reactions were set up using QX200 ddPCR EvaGreen Supermix (Bio-Rad, Hercules, CA, USA), with 100 nM of forward and reverse primer in an end volume of 22 µl. Between 15,000 and 20,000 droplets were generated using an AugoDG droplet generator and DG32 cartridges (Bio-Rad). PCR was then performed as follows: 10 min denaturation at 95°C followed by 40 cycles of 30 sec at 94°C and 1 min at 58 °C. The reactions were ended for 5 min at 4°C, 5 min at 90°C and then cooled to 10°C. The ramp rate for all steps was 2°C/sec. Droplets were quantified using the QX200 droplet reader (Bio-Rad) and analysed with QuantaSoft analysis software (Bio-Rad). Expression was normalized to reference gene expression level, and copies of target transcript per µl are reported.

RESULTS

AONs lead to upregulation of the antiviral enzyme Oasl2

A total dose of 200 µg AON administered ICV did not result in any negative effect on the bodyweights of the mice in the FVB test cohort (Fig. 1B). However, in the C57Bl/6 validation cohort a significantly reduced bodyweight was observed already after 100 µg of AON, which persisted until the end of the study (Fig. S1). Despite this, epileptic seizures were sporadically observed directly after AON administration in our FVB test cohort, but not the C57Bl/6 validation cohort. This observation is consistent with previous reports of increased sensitivity to epileptic seizures in mice of FVB background [33]. Immunohistological staining for the PS backbone revealed widespread AON distribution throughout the isolated brain regions (Fig. 1C). Striatum, cortex and cerebellum tissue from mice treated ICV with either AON or PBS was collected for RNA sequencing (Fig. 1A).When analysing the 8 weeks (215 µg) and 2 weeks (665 µg) AON treatment groups from the FVB test cohort, no major differences in gene expression

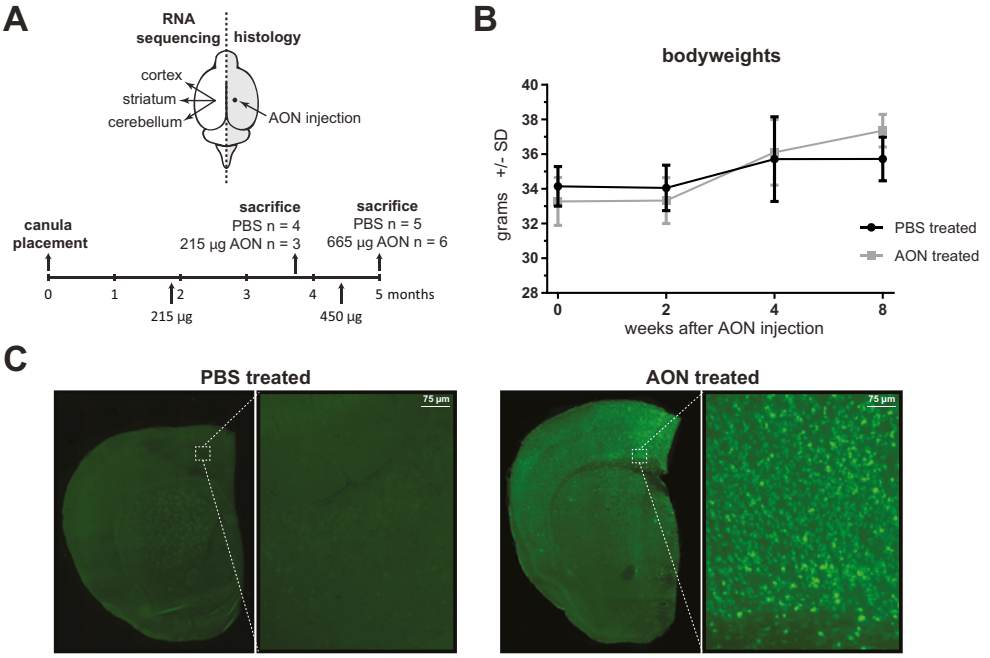

Figure 1. Study design and AON cellular uptake. A) During a 5 month period, FVB mice of the test cohort were injected intracerebroventricularly with a total of 215 µg AON (achieved with a total of 6 injections) or 625 µg AON (achieved with 2 additional injections). Two and 8 weeks after the last injection, mice were sacrificed and the right hemisphere was fixed for histology. Cortex, striatum and cerebellum were isolated from the left hemisphere for molecular analyses. **B**) Intracerebroventricular AON injection did not result in altered bodyweight compared to PBS injected mice in the FVB test cohort. Data depicted from mice treated with 215 µg AON (n = 4) or PBS (n = 5). **C**) Histological analysis showing AON distribution throughout the brain 2 weeks after the last injection.

were found between these dosage groups. For this reason it was decided to combine the 2- and 8 week time points groups for analysis of differential gene expression to obtain increased power for the comparison AON versus PBS treated. After exclusion of samples with low number of reads, poor alignment, or outliers in principal component analysis (Fig. S2A), a total of 44 samples were included for analysis of differential gene expression (Table 1). A median of 7.9 million reads per sample were aligned to the mouse reference genome (GRCm38/mm10). Genes with low expression (CPM < 4) were excluded, leading to inclusion of 12,160 genes for differential gene expression analysis. None of the mouse genes containing >16 nucleotide homology in BLAST[34] analysis were observed to be downregulated in the RNA sequencing analysis.

Gene expression analysis revealed a total of 925 genes differentially expressed (FDR <0.05) in at least one brain region of animals treated with AON. The top 10 differentially expressed genes and corresponding fold changes per brain region are depicted in Table 2. The largest and most consistent change observed for each brain region was an upregulation of 2'-5'-oligoadenylate synthase-like protein 2 *(Oasl2)* (Fig. 2A), which is an dsRNA-activated antiviral enzyme

Table 2. Top 10 significantly altered gene expression in brain after AON treatment

Gene	Name	FDR	Cerebellum log2 fold change	Cortex log2 fold change	Striatum log2 fold change	Protein function
Oasl2	2'-5'-oligoadenylate synthase-like protein 2	1.3E-07	2.2*	1.9	2.5*	Interferon-induced, dsRNA-activated antiviral enzyme
Sphkap	A-kinase anchor protein SPHKAP	1.3E-07	0.1	0.3	-0.9*	regulation of protein kinase A signaling
Lgals3bp	Galectin-3-binding protein	1.9E-07	1.4	1.5*	1.3*	scavenger receptor activity
Bst2	Bone marrow stromal antigen 2	1.2E-06	1.3	2.0	2.7*	defence response to virus
H2-Q4	Histocompatibility 2, Q region locus 4	3.9E-06	0.9	0.9	1.8*	antigen processing and presentation of peptide antigen via MHC class I
Ifit3	Interferon-induced protein with tetratricopeptide repeats 3	4.3E-06	1.4	1.4	1.8*	cellular response to interferon-alpha
Kcns1	Potassium voltage-gated channel subfamily S member 1	5.6E-06	0.0	-0.4	1.9*	potassium ion transport
Dgat2	Diacylglycerol O-acyltransferase 2	5.8E-06	0.1	0.2	0.9*	triacylglycerol biosynthesis
Kctd9	BTB/POZ domain-containing protein KCTD9	6.8E-06	-0.3	-0.1	-0.8*	adapter of E3 ubiquitin-protein ligase complex
Vipr1	Vasoactive intestinal polypeptide receptor 1	7.3E-06	-0.1	0.2	1.5*	cell surface receptor signalling pathway

* = gene is differentially expressed within individual brain region

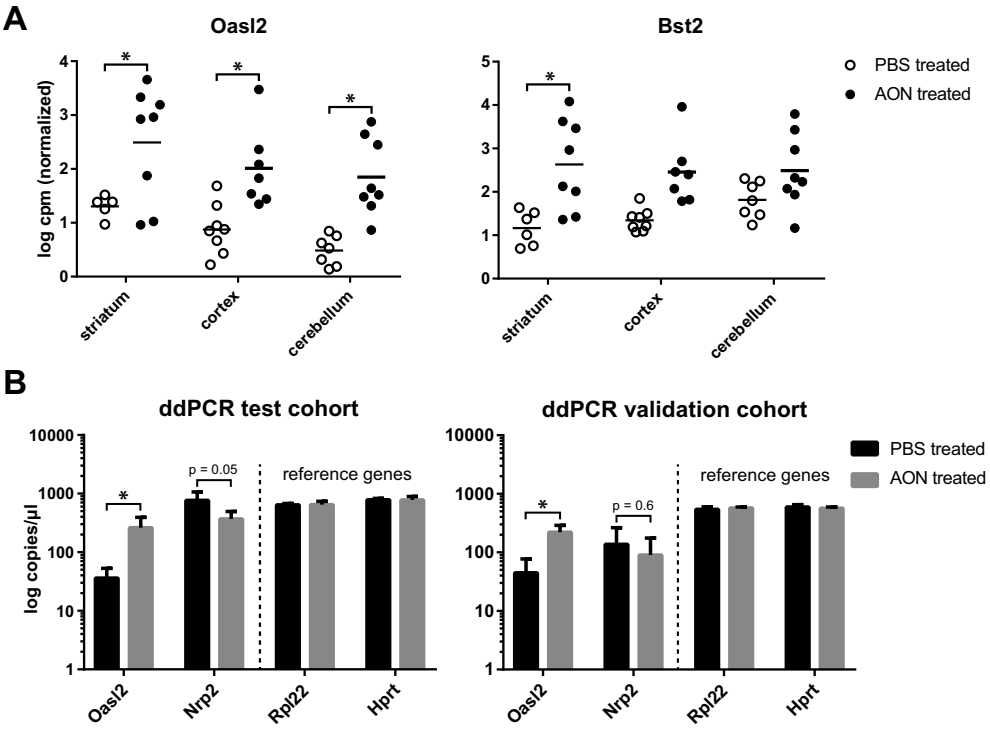

Figure 2. Increased expression of *Oasl2* in brain of AON treated mice. A) RNA sequencing shows expression of *Oasl2* and *Bst2* most strongly upregulated in response to AON, in particular in the striatum. * = FDR < 0.05, based on 8 vs 8 mice, analysis on samples of 2 weeks and 8 weeks after AON injection. **B**) ddPCR validation of top upregulated (*Oasl2*) and top downregulated (*Nrp2*) genes in striatum at 2 weeks after AON injection (FVB test cohort), and 4 months after AON injection (C57Bl/6 independent validation cohort). Based on ddPCR of 4 vs 4 mice. * = $p < 0.05$ using student's t-test.

involved in the innate antiviral response. Oasl2 requires double-stranded RNA as a co-factor [35], though the enzyme does not have a characteristic dsRNA binding motif [36].

Other top differentially upregulated genes were also involved in the immune and anti-viral response, such as Bone marrow stromal antigen 2 (*Bst2),* Histocompatibility 2, Q region locus 4 *(H2-Q4)* and Interferon-induced protein with tetratricopeptide repeats 3 *(Ifit3)*. In general, the upregulation of these genes was observed to a larger extent in the striatum than in the cortex and cerebellum, and were altered at both the 2 and 8 week time points after AON injection. Since AON uptake is comparable between striatum and cortex, it is unlikely that this difference is due to uptake efficiency of the AON. The top upregulated (*Oas*l2*)* and a downregulated (*Nrp2*) gene was validated using ddPCR on the same striatum RNA as was used for RNA sequencing. Both transcripts showed similar expression differences as detected in the RNA sequencing analysis, with *Oasl2* showing strong significant upregulation in AON treated mice (log2FC = 2.87) and *Nrp2* showing significant downregulation (log2FC = -1.05). A similar upregulation of

Oasl2 (Fig 2B) and several other immune system associated genes (Table S2) was also confirmed in the C57Bl/6 validation cohort through ddPCR. The immunostimulatory effect of the AON appears to be long lasting since mice of the validation cohort were sacrificed 4 months after the last AON administration (Fig. S1) and seems to be independent of the genetic background of the mice.

Immune system pathways are activated in AON treated brain

To determine which biological processes are altered in the mouse brain in response to AON administration, we performed pathway analysis using Ingenuity [37] and DAVID [38] on the significantly altered genes with FDR < 0.01 observed in the RNA sequencing analysis. This approach led to inclusion of 379 genes with relatively large changes that showed a most consistent change across the three brain regions. The significant canonical pathways and biological processes (KEGG) that are altered in response to the AON are listed in Table 3. Pathways involving the immune system, such as interferon and B-cell receptor signalling were activated in the AON treated mice.

Examination of the biological processes with DAVID showed that the most significant alteration in immune system associated genes. This process included 11 differentially expressed genes that were most strongly upregulated in striatum (Fig. 3). We validated 5 of these genes through ddPCR, (Fig. 2B and Table S2) which confirmed upregulation of the immune system associated genes *Oasl2, Ifit3, Bst2*, *Trim25* and *Lgals3bp* genes in striatum of AON treated mice in both the FVB test- and C57Bl/6 validation cohort. Together, these upregulated genes point to an innate immune response and complement activation, which constitutes the immediate defense in response to potential pathogens. In the context of the brain, this would suggest

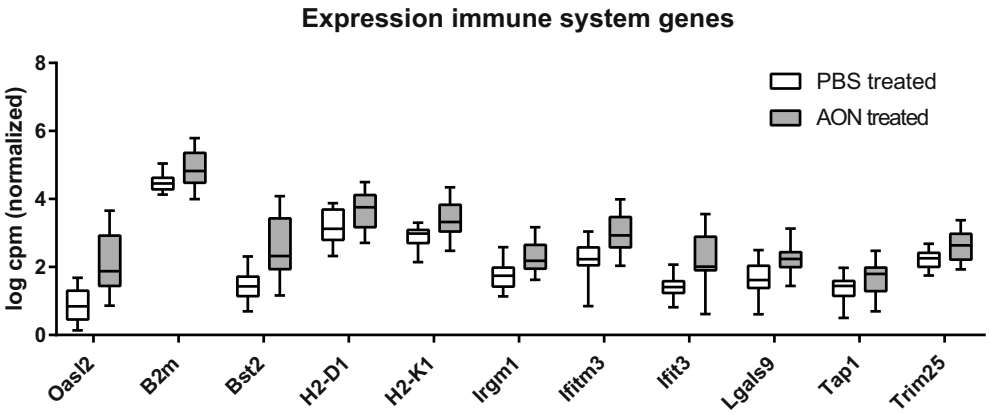

Figure 3. Immune system associated genes are upregulated in brain after AON injection. Expression of 11 significantly altered genes in brain belonging to immune system process (GO:0002376). Based on RNA sequencing analysis of cortex, cerebellum and striatum from 9 PBS treated vs 9 AON treated animals.

Table 3. Pathways and biological processes altered after AON treatment

	Number of genes	FDR	Activation z-score
Pathway (Ingenuity)			
Interferon Signaling	5	3.2E-04	2.0
G-Protein Coupled Receptor Signaling	13	7.9E-04	NA
GABA Receptor Signaling	6	1.1E-03	NA
B Cell Receptor Signaling	10	1.5E-03	2.3
IGF-1 Signaling	7	2.1E-03	NA
Leukocyte Extravasation Signaling	10	3.2E-03	2.3
Neuropathic Pain Signaling In Dorsal Horn Neurons	7	3.4E-03	1.9
Complement System	4	3.4E-03	2.0
Biological process (KEGG)	**Number of genes**	**FDR**	**Identifier**
Immune system process	11	2.8E-05	GO:0002376
Cellular response to interferon-beta	5	5.2E-04	GO:0035456
Antigen processing and presentation of peptide antigen via MHC class I	4	2.6E-03	GO:0002474
Defense response to virus	6	0.01	GO:0051607
Innate immune response	7	0.03	GO:0045087

microglia involvement. For this reason, we next performed histological analysis of microglial activation.

Microglia activation and increased astrocyte density

Based on the transcriptomic analysis, administration of the AON resulted in an immunologic response most strongly in the striatum of the mice. To further assess this innate immune response, immunohistological staining was performed on brain sections for the microglia marker allograft inflammatory factor 1 (Aif1) and for the astrocyte marker glial fibrillary acidic protein (GFAP). Microglia are brain resident macrophages that are widely expressed in the brain and constitute a major component of the innate arm of the brain immune system [39, 40]. In the RNA sequencing analysis, *Aif1* expression was significantly increased in the AON treated mouse brain. Mean optical density measurements in striatum did not reveal a significant change in the Aif1 levels in AON treated mice (Fig. 4B), indicating no significant increase in the number of microglia cells. However, when more closely examining the number of activated and resting state cells, an increase in activated microglia was observed in striatum of AON treated mice (Fig. 4C), similar to previously reported for CpG-containing AONs [41].

RNA sequencing results did not show significant alteration of *GFAP* transcript levels in AON treated mice. However, staining of GFAP in AON treated animals did reveal a small significant increase in mean optical GFAP density in striatum (Fig. 4B). GFAP is a marker for reactive astrocytes, which is a common cell type of the CNS with a wide range of functions.

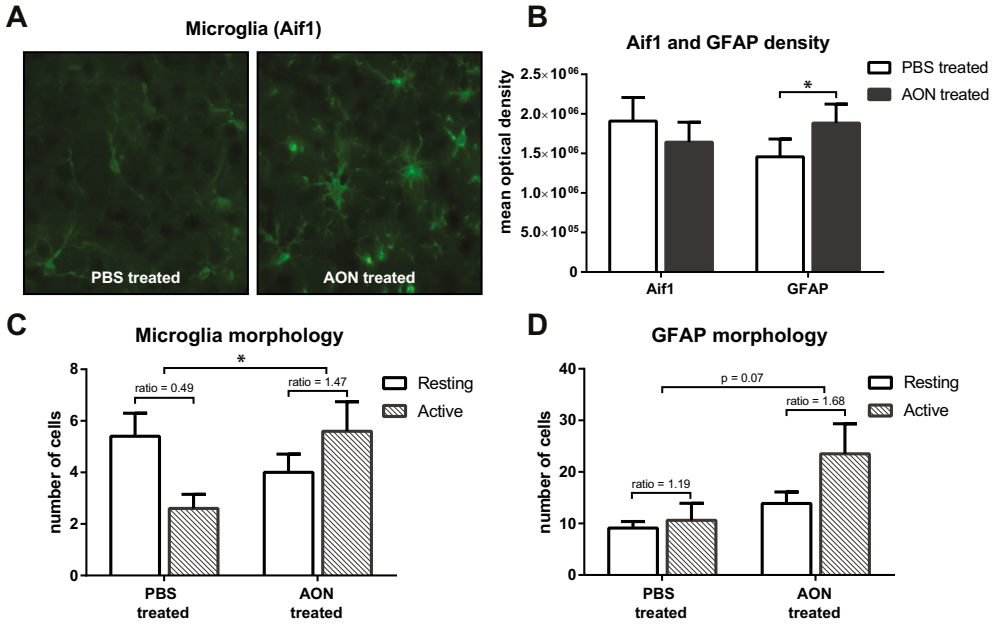

Figure 4. Assessment of astrocyte and microglia markers in striatum. Histological analysis of the microglia marker Aif1 and astrocyte marker GFAP was performed on 3 coronal striatum sections per mouse. **A**) Representative example of microglia staining with Aif1 of a PBS and AON treated mouse at 40x magnification. **B**) Quantification of the optical density revealed no observable change in Aif1 levels, but did show a significantly increased level of GFAP. **C**) Despite no increased number of Aif1 positive cells, the ratio of active to resting state microglia was significantly increased in striatum of AON treated mice. **D**) Scoring of GFAP morphology showed a general increase in astrocytes in AON treated mice, and a trend towards increased ratio of active over resting state cells. Based on 3 sections per mouse from 5 vs 5 mice. * $p < 0.05$ with student's t-test.

Astrocytes express Toll-like receptors (TLR) and are capable of producing several cytokines and chemokines [42]. Reactive astrogliosis is often a response to cytokines such as TGF-α or through indirect activation via neurons, microglia or endothelial cells [43]. When examining the activity state of astrocytes in the striatum, an increase in the number of active glia cells was observed in AON treated mice (Fig. 4D). To determine whether the immune stimulatory effect was not restricted to a single AON sequence, additional immunohistological stainings of brain tissue from a previous mouse study (described in [24]) was used. This AON was also a 2-'O-methyl PS-AON and was complementary to both the murine and human huntingtin mRNA, but showed no effect on the murine huntingtin transcript [24]. Similar to the AON used in the present study, this second AON resulted in increased astrocyte and microglia activation in the striatum of AON treated mice (Fig. S3), suggesting that the immune stimulation reported here is not restricted to a single AON sequence.

DISCUSSION

AONs are increasingly being used for treatment of CNS disorders, and have recently received FDA approval for treatment of SMA [44]. In this study we set out to determine the side effects of a uniformly modified 2-'O-methyl PS-AON in the mouse brain. This type of AON is typically implemented in steric blocking applications, such as exon inclusion or exon skipping [3].

The AON did not contain CpG motifs, which are known to be potent immunostimulatory agents [45]. A bolus ICV injection led to widespread distribution and cellular uptake throughout the mouse brain, in line with previous reports using similar AON chemistries [4, 6, 26]. Despite using the same AON, we observed different effects on bodyweight in our FVB test and C57Bl/6 validation cohort of mice. Mice in the validation cohort showed a reduction in bodyweight already after 100 µg ICV administration of AON, whilst our test cohort showed no discernible difference in bodyweight at a dose of 615 µg AON. This disparity may be the result of differences between the FVB and C57Bl/6 mouse background, or the differences in dosing schedule between the two cohorts.

Through RNA sequencing analysis, we found that the AON led to upregulation of several transcripts associated with the immune system. The largest upregulation was observed for *Oasl2*, *Bst2*, *Ifit3* and *H2-Q4*. These genes were upregulated in all brain regions tested (striatum, cortex and cerebellum), and generally showed a slightly larger fold change in the striatum compared to cortex and cerebellum. Given comparable AON uptake in striatum and cortex, this suggests the striatum is more sensitive to the immunostimulatory effects of the AON. The top differentially expressed genes were also found upregulated in the C57Bl/6 validation cohort, indicating that the immune system activation is not dependent on the genetic background of the mice.

It has been found that particular AON sequences, even without CpG motifs, can result in an atypical inflammatory response [46]. It is therefore important to consider that the immune stimulatory effects we describe here can potentially be confounded by the specific sequence of the AON used. However, we have confirmed the microglia and astrocyte activation for a different AON sequence of identical chemistry (Fig. S3), indicating that the results described here are not unique to one sequence.

The most strongly upregulated gene in response to the AON, *Oasl2,* belongs to the 2',5'-oligoadenylate synthetase gene family, of which a total of 11 have been identified in mouse, compared to 4 in human [47]. In the mouse brain, *Oasl2* is the most highly expressed of the enzyme family [47] and is an antiviral enzyme which through oligoadenylate synthetase activity activates ribonucleases, resulting in degradation of viral RNA. Oasl is one of the proteins upregulated in response to type I and II interferon (IFN) cytokines, and confers resistance to viral infection [48]. In response to virus infection, IFN induced upregulation of Oas activates the ribonuclease L, which leads to RNA degradation [49].

The second most upregulated gene observed in AON treated mice, the transmembrane protein *Bst2,* is also an IFN induced protein. Similar to Oasl2, Bst2 is a component of the innate defence response to viruses [50]. Bst2 is also known as tetherin, because it was identified as

a protein that caused retention of virions on infected cell surfaces [51]. Bst2 is able to tether these virions based on recognition of pathogen-associated molecular patterns (PAMPs), but is also able to act as a pattern-recognition receptor capable of signalling to the immune system through NFκB-dependent proinflammatory gene expression [52]. Indeed, double-stranded RNA is a known PAMP recognized by TLR3, which upon activation results in NF-κB and IFN-beta production [53]. Surprisingly however, Bst2 showed negligible ability to induce NF-κB response [52], suggesting this downstream signalling pathway may not have been activated in the mouse brain here. In line with this, we did not observe significant alteration in expression levels of *NFKB1* between PBS and AON treated mice. The increase in *Bst2* expression in this study (Log2FC = 2) is not substantially different from what was previously observed in transcriptional analysis of a mouse centrally injected with lippolysaccharide (LPS), where *Bst2* showed a Log2FC of 2.82 [54]. This observation indicates that the immune activation in response to the AON can be quite substantial at the dosages tested here, although expression changes of other immune response genes are more mildly affected in our study compared to LPS injection [54].

Another strongly upregulated gene in brain of the AON treated mice was *Ifit3*. Similar to Oasl2 and Bst2, Ifit3 is an anti-viral protein that is upregulated in response to IFN signalling [55]. Ifit3 restricts DNA and RNA virus replication, and evidence suggests that the Ifit family of proteins plays an important role in destruction of invasive RNA [56]. Ifit proteins are able to bind viral RNA and sequester viral proteins in the cytoplasm [57]. The observation that several IFN induced genes are upregulated in response to the AON suggest that the innate immune system is activated in response to the AON, resulting in IFN signalling. In line with this, we observed microglia activation based on significant *Aif1* transcript upregulation in RNA sequencing analysis, as well as increased active state microglia cells in histological examination. These observations are in concordance with previous reports, where doses higher than 100 μg of 2-'O-methyl PS-AON led to significant *Aif1* transcript upregulation [6]. Similarly, the observed increase in astrocyte activation in this study is indicative of a neuroprotective response in response to the AON [58]. Though the role of reactive astrocytes is still not well understood, it was recently found that A1 reactive astrocytes are induced by cytokines originating from activated neuroinflammatory microglia [59]. The observed astrocyte activation in striatum of AON treated mice may thus be a downstream result of microglial activation.

The mechanisms underlying the immune activation by RNA and AONs has been previously investigated, and a large portion of the immune activation originates from TLR stimulation (reviewed in [60]). This activation can be antagonized upon 2'-O-methylation of RNA [61, 62], which strongly reduces the immunostimulatory effects of the AON. Nonetheless, even in absence of CpG motifs and having 2'-metoxyethyl modifications, AONs are still capable of inducing an immune response [63]. In particular TLR3, 7 and 8 were shown to recognize single-stranded RNA [64-66]. Though the majority of TLRs sense stimulatory components on the cell surface, TLR3, 7 and 8 sense nucleic acids in endosomal compartments of the cell [65]. These three TLRs are expressed in microglia of mice [67], whilst astrocytes in contrast only express low levels of TLR2, 4, 5 and 9 in resting state [68]. This argues for an initiatory role of the microglia, which are able to sense the AONs through their TLRs, resulting in cytokine production and downstream

activation of the astrocytes. However, it is also known that human neurons express TLR3 [69] and TLR8 [70], and are able to initiate an anti-viral response characterized by cytokines (TNF-alpha, IL6), chemokines (CCL-5, CXCL-10) and antiviral molecules 2'5'OAS and IFN-beta [69].

Of note, the TLR receptors and general immune response is known to differ between mouse and human [71, 72]. For instance, CpG stimulatory sequences do not elicit TLR9 dependent TNF-alpha dependent toxicity in humans after pulmonary administration, while they do in mice [73]. This difference was hypothesized to be due to differential TLR9 expression patterns between rodents and primates, as monocyte/macrophage cells do not express TLR9 in primates [73]. Further, small interfering RNA (siRNA) was shown to be a ligand for the murine TLR3, whereas the human TLR3 was unresponsive to the siRNA [74]. It may therefore be difficult to extrapolate the murine immune response for AONs to the human situation.

However, also the use of monkeys as a model for AON tolerability has presented difficulties, as monkeys have a greater sensitivity to complement activation in response to second generation AONs compared to humans [75, 76]. As such, mouse models may overestimate the contribution of AON sequence specific effects, whilst experiments in monkeys appear to overestimate the AON induced complement activation aspect.

In conclusion, we show here that a 2-'O-methyl PS-AON of 19 nucleotide in length results in mild activation of the innate immune response when administered to the mouse brain. The immune activation is characterized by increased activation of microglia and astrocytes, likely resulting in IFN signalling. The resulting transcriptional changes in the brain are most strongly identified by upregulation of *Oasl2* and *Bst2*.

ACKNOWLEDGEMENTS

The authors want to thank Bharath Sampadi for performing Ingenuity analysis, Melvin Evers for advice on study design, Frank Rigo for providing antibody reagents, Peter-Bram 't Hoen and Szymon Kielbasa for advice on RNA sequencing analysis, and Ólafur Magnússon (Decode Genetics) for performing the RNA sequencing.

AUTHOR DISCLOSURE STATEMENT

The authors declare no competing financial interests.

REFERENCES

1. Lundin, KE, Gissberg, O, and Smith, CI (2015). Oligonucleotide Therapies: The Past and the Present. *Human gene therapy* **26**: 475-485.
2. Khvorova, A, and Watts, JK (2017). The chemical evolution of oligonucleotide therapies of clinical utility. *Nature biotechnology* **35**: 238-248.
3. Evers, MM, Toonen, LJ, and van Roon-Mom, WM (2015). Antisense oligonucleotides in therapy for neurodegenerative disorders. *Advanced drug delivery reviews* **87**: 90-103.
4. Casaca-Carreira, J, Temel, Y, Larrakoetxea, I, and Jahanshahi, A (2017). Distribution and Penetration of Intracerebroventricularly Administered 2'OMePS Oligonucleotide in the Mouse Brain. *Nucleic Acid Ther* **27**: 4-10.
5. Juliano, RL (2016). The delivery of therapeutic oligonucleotides. *Nucleic Acids Res* **44**: 6518-6548.
6. Rigo, F, Chun, SJ, Norris, DA, Hung, G, Lee, S, Matson, J, *et al.* (2014). Pharmacology of a central nervous system delivered 2'-O-methoxyethyl-modified survival of motor neuron splicing oligonucleotide in mice and nonhuman primates. *The Journal of pharmacology and experimental therapeutics* **350**: 46-55.
7. Chiriboga, CA (2017). Nusinersen for the treatment of spinal muscular atrophy. *Expert review of neurotherapeutics*: 1-8.
8. Hua, Y, Sahashi, K, Hung, G, Rigo, F, Passini, MA, Bennett, CF, *et al.* (2010). Antisense correction of SMN2 splicing in the CNS rescues necrosis in a type III SMA mouse model. *Genes Dev* **24**: 1634-1644.
9. Kordasiewicz, HB, Stanek, LM, Wancewicz, EV, Mazur, C, McAlonis, MM, Pytel, KA, *et al.* (2012). Sustained therapeutic reversal of Huntington's disease by transient repression of huntingtin synthesis. *Neuron* **74**: 1031-1044.
10. Smith, RA, Miller, TM, Yamanaka, K, Monia, BP, Condon, TP, Hung, G, *et al.* (2006). Antisense oligonucleotide therapy for neurodegenerative disease. *The Journal of clinical investigation* **116**: 2290-2296.
11. Miller, TM, Pestronk, A, David, W, Rothstein, J, Simpson, E, Appel, SH, *et al.* (2013). An antisense oligonucleotide against SOD1 delivered intrathecally for patients with SOD1 familial amyotrophic lateral sclerosis: a phase 1, randomised, first-in-man study. *Lancet Neurol* **12**: 435-442.
12. Sharma, VK, Sharma, RK, and Singh, SK (2014). Antisense oligonucleotides: modifications and clinical trials. *MedChemComm* **5**: 1454-1471.
13. Levin, AA (1999). A review of the issues in the pharmacokinetics and toxicology of phosphorothioate antisense oligonucleotides. *Biochimica et biophysica acta* **1489**: 69-84.
14. Brown, DA, Kang, SH, Gryaznov, SM, DeDionisio, L, Heidenreich, O, Sullivan, S, *et al.* (1994). Effect of phosphorothioate modification of oligodeoxynucleotides on specific protein binding. *The Journal of biological chemistry* **269**: 26801-26805.
15. Guvakova, MA, Yakubov, LA, Vlodavsky, I, Tonkinson, JL, and Stein, CA (1995). Phosphorothioate oligodeoxynucleotides bind to basic fibroblast growth factor, inhibit its binding to cell surface receptors, and remove it from low affinity binding sites on extracellular matrix. *The Journal of biological chemistry* **270**: 2620-2627.
16. Galbraith, WM, Hobson, WC, Giclas, PC, Schechter, PJ, and Agrawal, S (1994). Complement activation and hemodynamic changes following intravenous administration of phosphorothioate oligonucleotides in the monkey. *Antisense research and development* **4**: 201-206.

17. Bjersing, JL, Eriksson, K, Tarkowski, A, and Collins, LV (2004). The arthritogenic and immunostimulatory properties of phosphorothioate oligodeoxynucleotides rely on synergy between the activities of the nuclease-resistant backbone and CpG motifs. *Inflammation* **28**: 39-51.

18. Elepfandt, P, Rupprecht, S, Schoning-Burkhardt, B, Volk, HD, and Woiciechowsky, C (2002). Oligodeoxynucleotides induce brain inflammation in rats when infused intracerebroventricularly. *Neuroscience letters* **322**: 107-110.

19. Meng, W, Yamazaki, T, Nishida, Y, and Hanagata, N (2011). Nuclease-resistant immunostimulatory phosphodiester CpG oligodeoxynucleotides as human Toll-like receptor 9 agonists. *BMC biotechnology* **11**: 88.

20. Henry, S, Stecker, K, Brooks, D, Monteith, D, Conklin, B, and Bennett, CF (2000). Chemically modified oligonucleotides exhibit decreased immune stimulation in mice. *The Journal of pharmacology and experimental therapeutics* **292**: 468-479.

21. Monteith, DK, Henry, SP, Howard, RB, Flournoy, S, Levin, AA, Bennett, CF, *et al.* (1997). Immune stimulation--a class effect of phosphorothioate oligodeoxynucleotides in rodents. *Anti-cancer drug design* **12**: 421-432.

22. Zhao, Q, Temsamani, J, Iadarola, PL, Jiang, Z, and Agrawal, S (1996). Effect of different chemically modified oligodeoxynucleotides on immune stimulation. *Biochemical pharmacology* **51**: 173-182.

23. Peng Ho, S, Livanov, V, Zhang, W, Li, J, and Lesher, T (1998). Modification of phosphorothioate oligonucleotides yields potent analogs with minimal toxicity for antisense experiments in the CNS. *Brain research Molecular brain research* **62**: 1-11.

24. Casaca-Carreira, J, Toonen, LJ, Evers, MM, Jahanshahi, A, van-Roon-Mom, WM, and Temel, Y (2016). In vivo proof-of-concept of removal of the huntingtin caspase cleavage motif-encoding exon 12 approach in the YAC128 mouse model of Huntington's disease. *Biomedicine & pharmacotherapy = Biomedecine & pharmacotherapie* **84**: 93-96.

25. Evers, MM, Tran, HD, Zalachoras, I, Meijer, OC, den Dunnen, JT, van Ommen, GJ, *et al.* (2014). Preventing formation of toxic N-terminal huntingtin fragments through antisense oligonucleotide-mediated protein modification. *Nucleic Acid Ther* **24**: 4-12.

26. Toonen, LJA, Rigo, F, van Attikum, H, and van Roon-Mom, WMC (2017). Antisense Oligonucleotide-Mediated Removal of the Polyglutamine Repeat in Spinocerebellar Ataxia Type 3 Mice. *Molecular therapy Nucleic acids* **8**: 232-242.

27. Shitaka, Y, Tran, HT, Bennett, RE, Sanchez, L, Levy, MA, Dikranian, K, *et al.* (2011). Repetitive closed-skull traumatic brain injury in mice causes persistent multifocal axonal injury and microglial reactivity. *Journal of neuropathology and experimental neurology* **70**: 551-567.

28. Brown, GC, and Neher, JJ (2010). Inflammatory neurodegeneration and mechanisms of microglial killing of neurons. *Molecular neurobiology* **41**: 242-247.

29. VanGuilder, HD, Bixler, GV, Brucklacher, RM, Farley, JA, Yan, H, Warrington, JP, *et al.* (2011). Concurrent hippocampal induction of MHC II pathway components and glial activation with advanced aging is not correlated with cognitive impairment. *Journal of neuroinflammation* **8**: 138.

30. Robinson, MD, and Oshlack, A (2010). A scaling normalization method for differential expression analysis of RNA-seq data. *Genome Biology* **11**: R25.

31. Robinson, MD, McCarthy, DJ, and Smyth, GK (2010). edgeR: a Bioconductor package for differential expression analysis of digital gene expression data. *Bioinformatics* **26**: 139-140.

32. Toonen, LJ, Schmidt, I, Luijsterburg, MS, van Attikum, H, and van Roon-Mom, WM (2016). Antisense oligonucleotide-mediated exon skipping as a strategy to reduce proteolytic cleavage of ataxin-3. *Sci Rep* **6**: 35200.

33. Goelz, MF, Mahler, J, Harry, J, Myers, P, Clark, J, Thigpen, JE, *et al.* (1998). Neuropathologic findings associated with seizures in FVB mice. *Laboratory animal science* **48**: 34-37.

34. Altschul, SF, Gish, W, Miller, W, Myers, EW, and Lipman, DJ (1990). Basic local alignment search tool. *Journal of molecular biology* **215**: 403-410.

35. Eskildsen, S, Justesen, J, Schierup, MH, and Hartmann, R (2003). Characterization of the 2'-5'-oligoadenylate synthetase ubiquitin-like family. *Nucleic Acids Res* **31**: 3166-3173.

36. Justesen, J, Hartmann, R, and Kjeldgaard, NO (2000). Gene structure and function of the 2'-5'-oligoadenylate synthetase family. *Cellular and molecular life sciences : CMLS* **57**: 1593-1612.

37. Kramer, A, Green, J, Pollard, J, Jr., and Tugendreich, S (2014). Causal analysis approaches in Ingenuity Pathway Analysis. *Bioinformatics* **30**: 523-530.

38. Huang da, W, Sherman, BT, and Lempicki, RA (2009). Systematic and integrative analysis of large gene lists using DAVID bioinformatics resources. *Nature protocols* **4**: 44-57.

39. Prinz, M, and Priller, J (2014). Microglia and brain macrophages in the molecular age: from origin to neuropsychiatric disease. *Nat Rev Neurosci* **15**: 300-312.

40. Filiano, AJ, Gadani, SP, and Kipnis, J (2015). Interactions of innate and adaptive immunity in brain development and function. *Brain research* **1617**: 18-27.

41. Dalpke, AH, Schafer, MK, Frey, M, Zimmermann, S, Tebbe, J, Weihe, E, *et al.* (2002). Immunostimulatory CpG-DNA activates murine microglia. *Journal of immunology (Baltimore, Md : 1950)* **168**: 4854-4863.

42. Carpentier, PA, Begolka, WS, Olson, JK, Elhofy, A, Karpus, WJ, and Miller, SD (2005). Differential activation of astrocytes by innate and adaptive immune stimuli. *Glia* **49**: 360-374.

43. Hol, EM, and Pekny, M (2015). Glial fibrillary acidic protein (GFAP) and the astrocyte intermediate filament system in diseases of the central nervous system. *Current opinion in cell biology* **32**: 121-130.

44. Aartsma-Rus, A (2017). FDA Approval of Nusinersen for Spinal Muscular Atrophy Makes 2016 the Year of Splice Modulating Oligonucleotides. *Nucleic Acid Ther* **27**: 67-69.

45. Dalpke, AH, Zimmermann, S, Albrecht, I, and Heeg, K (2002). Phosphodiester CpG oligonucleotides as adjuvants: polyguanosine runs enhance cellular uptake and improve immunostimulative activity of phosphodiester CpG oligonucleotides in vitro and in vivo. *Immunology* **106**: 102-112.

46. Burel, SA, Machemer, T, Ragone, FL, Kato, H, Cauntay, P, Greenlee, S, *et al.* (2012). Unique O-methoxyethyl ribose-DNA chimeric oligonucleotide induces an atypical melanoma differentiation-associated gene 5-dependent induction of type I interferon response. *The Journal of pharmacology and experimental therapeutics* **342**: 150-162.

47. Kakuta, S, Shibata, S, and Iwakura, Y (2002). Genomic structure of the mouse 2',5'-oligoadenylate synthetase gene family. *Journal of interferon & cytokine research : the official journal of the International Society for Interferon and Cytokine Research* **22**: 981-993.

48. Chebath, J, Benech, P, Revel, M, and Vigneron, M (1987). Constitutive expression of (2'-5') oligo A synthetase confers resistance to picornavirus infection. *Nature* **330**: 587-588.

49. Silverman, RH (2007). Viral encounters with 2',5'-oligoadenylate synthetase and RNase L during the interferon antiviral response. *Journal of virology* **81**: 12720-12729.

50. Tokarev, A, Skasko, M, Fitzpatrick, K, and Guatelli, J (2009). Antiviral activity of the interferon-induced cellular protein BST-2/tetherin. *AIDS research and human retroviruses* **25**: 1197-1210.

51. Neil, SJ, Zang, T, and Bieniasz, PD (2008). Tetherin inhibits retrovirus release and is antagonized by HIV-1 Vpu. *Nature* **451**: 425-430.

52. Galão, Rui P, Le Tortorec, A, Pickering, S, Kueck, T, and Neil, Stuart JD (2012). Innate Sensing of HIV-1 Assembly by Tetherin Induces NFκB-Dependent Proinflammatory Responses. *Cell Host & Microbe* **12**: 633-644.

53. Matsumoto, M, Kikkawa, S, Kohase, M, Miyake, K, and Seya, T (2002). Establishment of a monoclonal antibody against human Toll-like receptor 3 that blocks double-stranded RNA-mediated signaling. *Biochemical and biophysical research communications* **293**: 1364-1369.

54. Bonow, RH, Aid, S, Zhang, Y, Becker, KG, and Bosetti, F (2009). The brain expression of genes involved in inflammatory response, the ribosome, and learning and memory is altered by centrally injected lipopolysaccharide in mice. *The pharmacogenomics journal* **9**: 116-126.

55. Schmeisser, H, Mejido, J, Balinsky, CA, Morrow, AN, Clark, CR, Zhao, T, *et al.* (2010). Identification of alpha interferon-induced genes associated with antiviral activity in Daudi cells and characterization of IFIT3 as a novel antiviral gene. *Journal of virology* **84**: 10671-10680.

56. Zhou, X, Michal, JJ, Zhang, L, Ding, B, Lunney, JK, Liu, B, *et al.* (2013). Interferon induced IFIT family genes in host antiviral defense. *International journal of biological sciences* **9**: 200-208.

57. Diamond, MS, and Farzan, M (2013). The broad-spectrum antiviral functions of IFIT and IFITM proteins. *Nat Rev Immunol* **13**: 46-57.

58. Pekny, M, Wilhelmsson, U, and Pekna, M (2014). The dual role of astrocyte activation and reactive gliosis. *Neuroscience letters* **565**: 30-38.

59. Liddelow, SA, Guttenplan, KA, Clarke, LE, Bennett, FC, Bohlen, CJ, Schirmer, L, *et al.* (2017). Neurotoxic reactive astrocytes are induced by activated microglia. *Nature* **541**: 481-487.

60. Dalpke, A, and Helm, M (2012). RNA mediated Toll-like receptor stimulation in health and disease. *RNA biology* **9**: 828-842.

61. Robbins, M, Judge, A, Liang, L, McClintock, K, Yaworski, E, and MacLachlan, I (2007). 2'-O-methyl-modified RNAs act as TLR7 antagonists. *Molecular therapy : the journal of the American Society of Gene Therapy* **15**: 1663-1669.

62. Sioud, M, Furset, G, and Cekaite, L (2007). Suppression of immunostimulatory siRNA-driven innate immune activation by 2'-modified RNAs. *Biochemical and biophysical research communications* **361**: 122-126.

63. Senn, JJ, Burel, S, and Henry, SP (2005). Non-CpG-containing antisense 2'-methoxyethyl oligonucleotides activate a proinflammatory response independent of Toll-like receptor 9 or myeloid differentiation factor 88. *The Journal of pharmacology and experimental therapeutics* **314**: 972-979.

64. Diebold, SS, Kaisho, T, Hemmi, H, Akira, S, and Reis e Sousa, C (2004). Innate antiviral responses by means of TLR7-mediated recognition of single-stranded RNA. *Science* **303**: 1529-1531.

65. Xagorari, A, and Chlichlia, K (2008). Toll-like receptors and viruses: induction of innate antiviral immune responses. *The open microbiology journal* **2**: 49-59.

66. Butchi, NB, Pourciau, S, Du, M, Morgan, TW, and Peterson, KE (2008). Analysis of the neuroinflammatory response to TLR7 stimulation in the brain: comparison of multiple TLR7 and/or TLR8 agonists. *Journal of immunology (Baltimore, Md : 1950)* **180**: 7604-7612.

67. Olson, JK, and Miller, SD (2004). Microglia initiate central nervous system innate and adaptive immune responses through multiple TLRs. *Journal of immunology (Baltimore, Md : 1950)* **173**: 3916-3924.

68. Bowman, CC, Rasley, A, Tranguch, SL, and Marriott, I (2003). Cultured astrocytes express toll-like receptors for bacterial products. *Glia* **43**: 281-291.

69. Lafon, M, Megret, F, Lafage, M, and Prehaud, C (2006). The innate immune facet of brain: human neurons express TLR-3 and sense viral dsRNA. *Journal of molecular neuroscience : MN* **29**: 185-194.

70. Ma, Y, Haynes, RL, Sidman, RL, and Vartanian, T (2007). TLR8: an innate immune receptor in brain, neurons and axons. *Cell cycle (Georgetown, Tex)* **6**: 2859-2868.

71. Bryant, CE, and Monie, TP (2012). Mice, men and the relatives: cross-species studies underpin innate immunity. *Open biology* **2**: 120015.

72. Ketloy, C, Engering, A, Srichairatanakul, U, Limsalakpetch, A, Yongvanitchit, K, Pichyangkul, S, *et al.* (2008). Expression and function of Toll-like receptors on dendritic cells and other antigen presenting cells from non-human primates. *Veterinary immunology and immunopathology* **125**: 18-30.

73. Campbell, JD, Cho, Y, Foster, ML, Kanzler, H, Kachura, MA, Lum, JA, *et al.* (2009). CpG-containing immunostimulatory DNA sequences elicit TNF-alpha-dependent toxicity in rodents but not in humans. *The Journal of clinical investigation* **119**: 2564-2576.

74. Weber, C, Muller, C, Podszuweit, A, Montino, C, Vollmer, J, and Forsbach, A (2012). Toll-like receptor (TLR) 3 immune modulation by unformulated small interfering RNA or DNA and the role of CD14 (in TLR-mediated effects). *Immunology* **136**: 64-77.

75. Shen, L, Frazer-Abel, A, Reynolds, PR, Giclas, PC, Chappell, A, Pangburn, MK, *et al.* (2014). Mechanistic understanding for the greater sensitivity of monkeys to antisense oligonucleotide-mediated complement activation compared with humans. *The Journal of pharmacology and experimental therapeutics* **351**: 709-717.

76. Henry, SP, Jagels, MA, Hugli, TE, Manalili, S, Geary, RS, Giclas, PC, *et al.* (2014). Mechanism of alternative complement pathway dysregulation by a phosphorothioate oligonucleotide in monkey and human serum. *Nucleic Acid Ther* **24**: 326-335.

SUPPLEMENTARY FIGURES

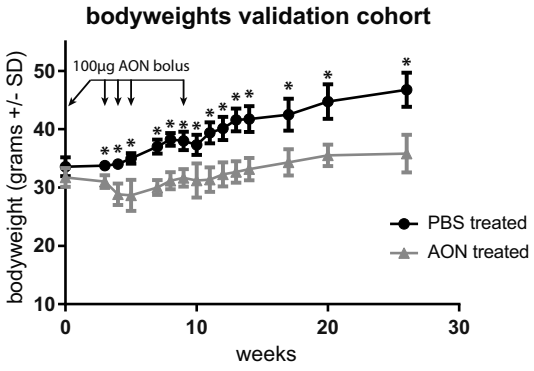

Supplementary Figure 1. Bodyweights of mice in validation cohort. C57BL/6 mice were injected intracerebroventricularly with a total of 500 µg AON during 10 weeks. Significantly reduced bodyweight was observed after each 100 µg AON injection. Mice were sacrificed approximately 4 months after the last AON injection for molecular analysis. Based on 4 PBS injected vs 8 AON injected mice.

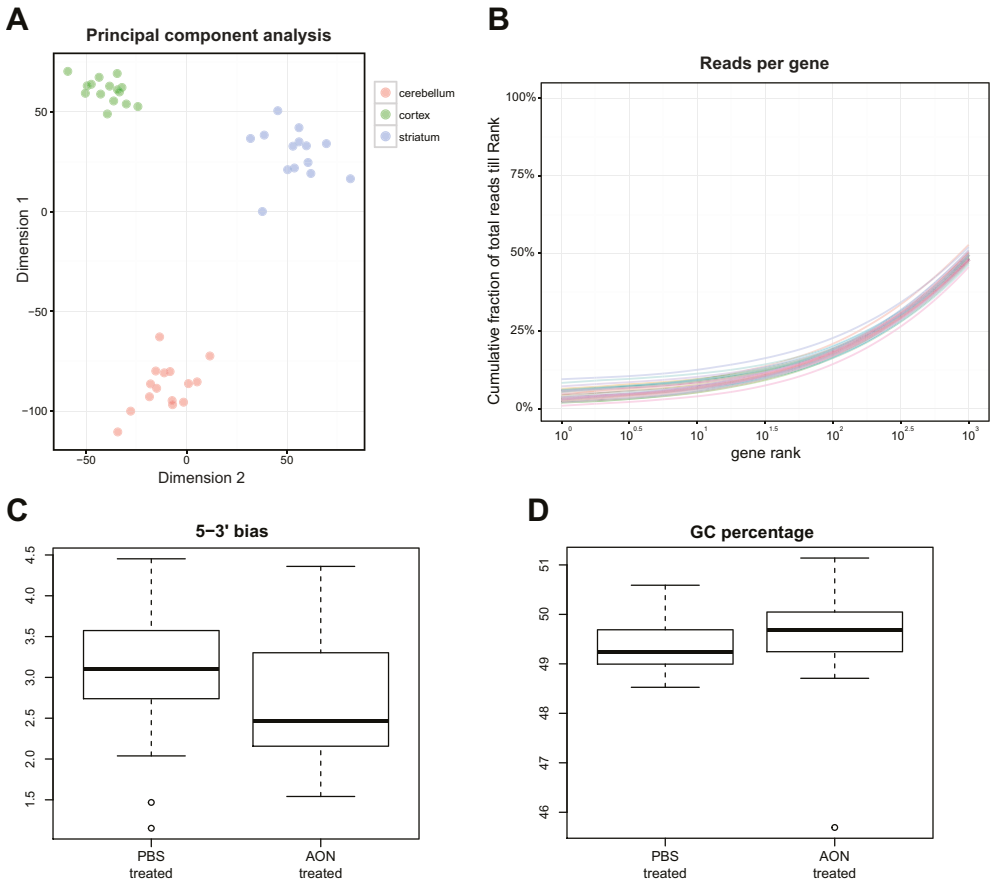

Supplementary Figure 2. RNA sequencing quality control. A) Principal component analysis was performed on normalized gene counts to determine clustering per brain region. Depicted is plot of samples used for differential gene analysis. B) Percentage of total reads per gene shows similar distribution for all 44 RNA sequencing samples. The first 1000 genes sorted on highest read counts are depicted, accounting for approximately 50% of total reads per sample. C) Average 5′ to 3′ read bias per treatment group. D) Average GC percentage of reads per treatment group.

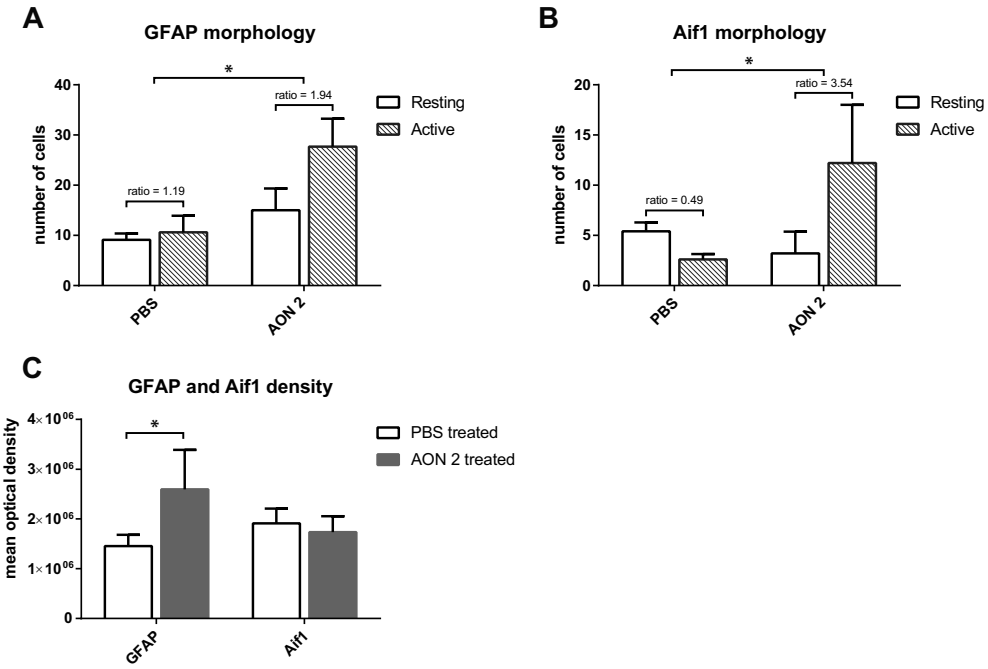

Supplementary Figure 3. Assessment of astrocyte and microglia markers in striatum of AON treated mice. Immunohistological staining was performed for an extra group of mice treated ICV with 665 µg of a different AON (AON 2) from a previous study [24]. AON 2 is also a fully PS backbone, 2'O-methyl modified 19-mer (sequence: GUCCCAUCAUUCAGGUCCAU), designed for splicing modulation of huntingtin, but was shown not to affect murine huntingtin [24]. The PBS treated group is identical as in figure 4. **A**) Based on GFAP based morphology scoring, a significantly increased ratio of activated astrocytes were present in striatum of AON 2 treated mice compared to PBS treated mice. **B**) Significantly increased levels of activated microglia were detected in striatum after treatment with AON 2. **C**) Optical density quantification showed increased levels of GFAP in striatum after AON 2 treatment. Based on 3 sections per mouse and 5 mice per treatment group. * $p < 0.05$ with student's t-test.

SUPPLEMENTARY TABLES

Supplementary Table 1. primers used for ddPCR and ddPCR

Target gene (mouse)	Primer name	Sequence (5′ to 3′)
Nrp2	mNrp2_ex9_fw	AGCCTAAATGGCAAGGACTG
Nrp2	mNrp2_ex10_rev	ATCGAACCTTCGGATGTCAG
Slfn5	mSlfn5_Qex4_Fw	ATGTGTGGAAGACCTGCAGAAG
Slfn5	mSlfn5_Qex5_Rev	AATCTGCGAAGAGGTCCTTG
Trim25	mTrim25_Qex4_Fw	ATGGCTCAGGTAACAAGGGAG
Trim25	mTrim25_Qex6_Rev	GGGAGCAACAGGGGTTTTCTT
Bst2	mBst2_Qex1_Fw	CACAGGCAAACTCCTGCAAC
Bst2	mBst2_Qex3_Rev	TGGTTCAGCTTCGTGACTTC
Ifit3	mIfit3_Qex1_Fw	TTTCCCAGCAGCACAGAAAC
Ifit3	mIfit3_Qex2_Rev	ACTTCAGCTGTGGAAGGATCG
Oasl2	mOASL2_Qex3_Fw	TGAAGAACCTCCTCCGGTTG
Oasl2	mOASL2_Qex4_Rev	TTTTGAGGGCAACACTGCAC
Lgals3bp	mLgals3bp_Qex1_Fw	TGCTGGTTCCAGGGACTCAA
Lgals3bp	mLgals3bp_Qex2_Rev	CCACCGGCCTCTGTAGAAGA
Hprt	mHprt_Qex6_fw	TCCCTGGTTAAGCAGTACAGCC
Hprt	mHprt_Qex7_rev	CGAGAGGTCCTTTTCACCAGC
Actb	mActb_Qex2_Fw	GGCTGTATTCCCCTCCATCG
Actb	mActb_Qex3_Rev	CCAGTTGGTAACAATGCCATGT
Rpl22	mRpl22ex3_fw1	AGGAGTCGTGACCATCGAAC
Rpl22	mRpl22ex3_rev1	TTTGGAGAAAGGCACCTCTG

Supplementary Table 2. Validation of expression changes in striatum

Gene	Log2FC RNA sequencing	Log2FC ddPCR test cohort	Log2FC ddPCR validation cohort
Slfn5	0.8	1.4	NT
Oasl	2.5	2.7	2.8
Ifit3	1.8	1.7	2.4
bst2	2.7	2.1	2.7
Trim25	0.8	1.0	1.2
Lgals3	1.3	0.9	1.4
Nrp2	-1.0	NT	-0.7

The Log2FC for the top differentially expressed genes in striatum of AON treated mice was validated using ddPCR using RNA from the test- and validation cohort. To allow for high throughput, cDNA from mice in the same treatment group were pooled. Test cohort: 4 PBS vs 6 AON treated mice. Validation cohort: 4 PBS vs 8 AON treated mice.